International Journal of the Physical Sciences Vol. 6(27), pp. 6303-6314, 2 November, 2011
Available online at http://www.academicjournals.org/IJPS
DOI: 10.5897/IJPS10.392
ISSN 1992 - 1950 ©2011 Academic Journals

Full Length Research Paper

A peg free hand shape authentication scheme with radon transform

Ahmed Mostayed and Sikyung Kim*

Department of Electrical Engineering, Kongju National University, Cheonan, Chungnam, South Korea.

Accepted 02 November, 2010

The hand shape authentication has been widely used on the biometrics field with an extensive range of potential applications since it is the well-suited with respect to security facility. The aim of this paper is to improve the accuracy and robustness of the hand based authentication system. In this paper, a hand shape authentication with a fixed angle radon transformation and a centroid scheme is proposed to achieve high accuracy and robustness with translation and rotation invariancy. Furthermore, the hand shape feature vector is developed using the radon transform with centroid to represent hand geometry, avoiding the more complicated and liable to errors of hand landmark extraction. This scheme can handle variability of hand's position, translation and rotation, especially in a peg free system with the help of centroid and radon transformation. The experimental results are promising and confirm the usefulness of the proposed approach for personal authentication by implementing the real hand geometry verification/identification system and it has proven to work effectively and competitively with low false acceptance and false rejection rates.

Key words: Hand shape authentication, radon transform, centroid, feature vector and biometric.

INTRODUCTION

Many physiological and behavioral characteristics of humans are typically invariant over time and unique to each individual. Those biometric features such as face, hand shape, fingerprint, palm-print, etc. have been proposed for the secured access control. The most widely studied biometrics has been fingerprint and hand because of the well-suited with respect to security facility. The reliability of hand biometrics has been hampered by the problems caused by pose, expression and illumination. Fingerprint is the most effective identification trait for decades now. However, it also has some limitations as a large group of users, elderly people and manual workers fail to deliver good quality fingerprint images. The surface area of fingerprints is quite small and any cuts or scar mark on this surface generates false minutiae, which undermines the integrity of the system (Kumar et al., 2006). As a result, other biometric traits are introduced and receiving increased interests. In recent works human gait and hand shape patterns have attracted many researchers. However, the simplicity of hand geometry has made it more favorable. Human hand can be characterized by its length, width, thickness, geometrical composition, shapes of the palm and shape and geometry of the fingers (Wong and Shi, 2002). The acquisition of hand image is a simple task with no special care needed for illumination or resolution. Moreover, low resolution hand image can be used for integrated hand geometry-palm print authentication system. High resolution hand images can be used in integrated identification/verification system in conjunction with fingerprints (Jain et al., 1997). Several patents (Sidlauskas, 1988; Jacoby et al., 1972; Miller, 1971; Ernst, 1971) have been issued for devices that measure hand geometry features for personal verify-cation. The devised system for personal authentication using bootstrap technique which effectively utilizes hand geometry features. A similar system using hand geometry features has been described in Han et al. (2002). Some related work using low-resolution digital hand images appears in (Jain et al., 1997; Gunther, 2002; Sanchez-Reillo et al., 2000; Oden et al., 2003).

Fixation pegs are used in these papers to restrict the hand movement and promising results were obtained.

*Corresponding author. E-mail: skim@kongju.ac.kr. Tel: 82-41-521-9155. Fax: 82-41-563-3689.

However, those may be biased by the small size of the database and an imposter can easily violate the integrity of system by using fake hand (Kumar et al., 2006; Gunther, 2002; Oden et al., 2003). An image set consisting of around 360 images were tested and a false acceptance rate (FAR) of 2% and a false rejection rate (FRR) of 15% were obtained. Gunther (2002), Oden et al. (2003) proposed a system for identification and verification using implicit polynomials. Combining their method with geometric features they achieved 95% success in identification and 99% success in verification. The training set they used consists of 40 images. Jain et al. (1999) developed a verification system based on alignment of finger contours and measured the mean alignment error between them. They experimented with 353 images from 50 persons and report FAR of 2% and FRR of 3.5%. Convenience acquisition systems along with good identification and verification performance has made hand geometry a popular biometric. Earlier works on hand shape was restricted to its length, width, thickness, geometrical composition, shapes of the palm and shape and geometry of the fingers for recognition with varying degrees of success. In typical methods pegs are almost always used to fix the placement of the hand and anatomical measurements are taken as features (Jain et al., 1997; Gunther, 2002; Jain et al., 1999). In Sanchez-Reillo et al. (2000) and Amayeh et al. (2006), the outline of the hand is extracted and is represented by a group of salient points, which serve as features in the verification process.

The objective of this paper is to propose a peg free and position invariant method for hand shape verification. The proposed scheme in this paper uses Radon Transform for extracting hand shape feature. One very significant anatomical feature of the hand palm is utilized in this method. The distance between center of mass of the hand palm and the boundary points on the hand is maximum at the middle finger tip. This fact is used to find the optimal parameter for Radon transform and one dimensional position invariant features are extracted from the binary hand silhouettes. The hand shape feature vector is developed using the radon transform with centroid to represent hand geometry, avoiding the more complicated and liable to errors of hand landmark extraction. This scheme can handle variability of hand's position, translation and rotation especially in a peg free system with the help of centroid and radon transformation. The experimental results are promising and confirm the usefulness of the proposed approach for personal authentication by implementing the real hand geometry verification/identification system, and it has proven to work effectively and competitively with low false acceptance and false rejection rates

PEG FREE HAND SHAPE AUTHENTICATION SCHEME

The peg free hand shape authentication scheme proposed in this paper uses the Radon Transform to extract position invariant feature vectors. The Radon transform is simply the line integral of an object on the image plane along all the lines from 0 to 360 degrees. However in this paper the radon Transform is taken along an optimal direction only. That optimal angle is found by locating the centroid of hand palm and subsequently locating middle finger tip. In this section several steps of the feature extraction process is described. The discussion begins with a brief introduction of radon Transform.

The Radon transform

The Radon Transform is named after the famous Austrian mathematician Johann Karl August Radon. One major application of Radon transform is CAT scan. It is also frequently used to detect lines in images. Radon transform of an image $f(x, y)$ for a given angle θ can be thought of as computing the projection of the image along that given angle. The resulting projection is a 1 D function which is the sum of the intensities of the pixels in that direction, or in other words a line integral. The Radon Transform of an image $f(x, y)$ for an angle θ is defined as

$$R(\rho,\theta) = \int_{-\infty}^{\infty}\int_{-\infty}^{\infty} f(x,y)\delta(\rho - x\cos\theta - y\sin\theta)\,dxdy \quad (1)$$

where (x, y) denotes spatial coordinates and ρ denotes the radial (perpendicular) distance from the coordinate origin to the line with angle θ. Relation of these parameters with spatial coordinate system is shown in Figure 1 (a). The Radon Transform of a line in spatial domain is a point in parameter domain. This property is used to detect lines in images (Hansen et al., 1996; Gonzalez et al., 2004). An example of such line detection is shown in Figure 1 b and c.

The Radon Transform possesses some important properties; these enable one to find Radon Transform of many functions in very simple ways. The most important properties are Linearity, Shifting and Rotation.

Linearity

$$\Re[af_1(x,y) + bf_2(x,y)] = a\Re[f_1(x,y)] + b\Re[f_2(x,y)] \quad (2)$$

Here $\Re[.]$ denotes Radon Transform operator. a and b are scalars.

Shifting

$$R[f(x - x_0, y - y_0)] = R(\rho - x_0\cos\theta - y_0\sin\theta, \theta) \quad (3)$$

That means shifting has only effect on the radial distance parameter. This property is later used to obtain shift invariant feature vectors.

Rotation

$$R[f(x', y')] = R(\rho, \theta - \phi) \quad (4)$$

where $x' = x\cos\phi + y\sin\phi, y' = -x\sin\phi + y\cos\phi$. ϕ

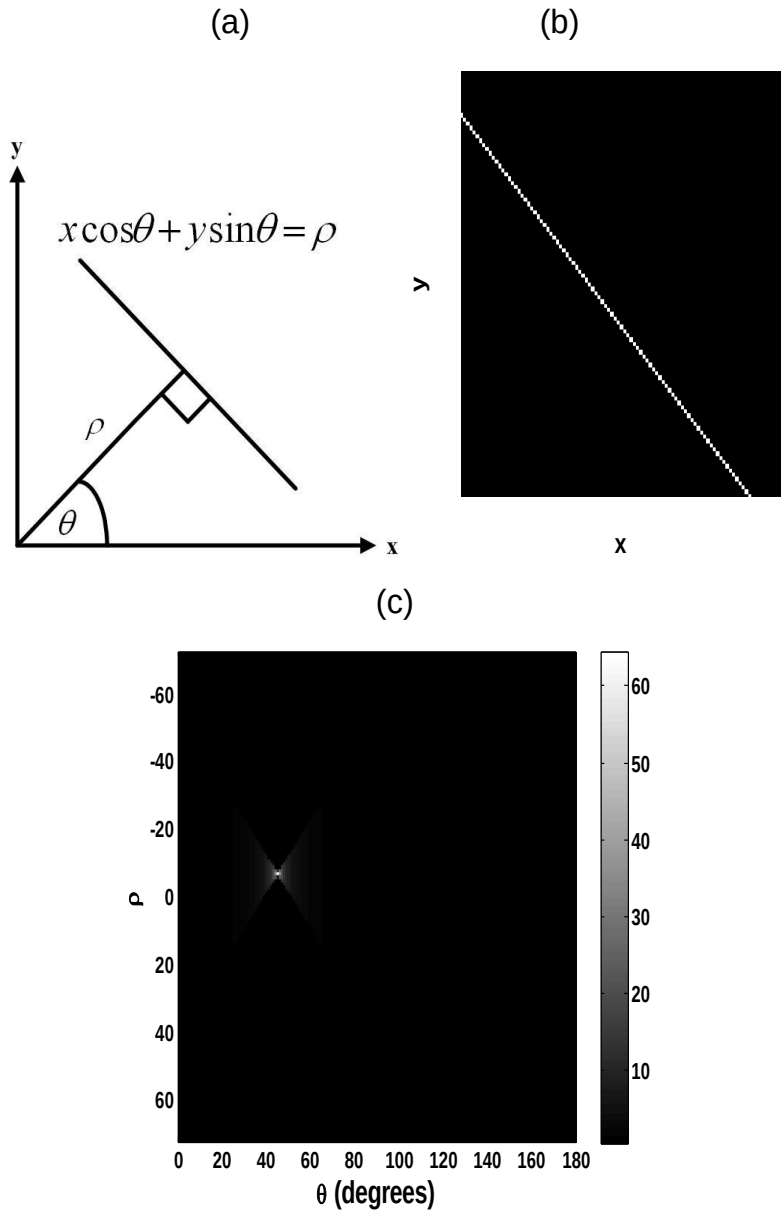

Figure 1 (a). Parameters for Radon transform. (**b**) A binary image consist of a line **(c**) Radon transform of that image. The bright spot indicates the line in parameter domain.

is the rotation angle. Note that the change is only on the angle parameter.

Hand image acquisition

The feature extraction process begins with the hand image acquisition. A document scanner was used to collect low resolution hand images against a dark background. 75 dpi images were taken in 8 bit gray scale format. Each image has a size of 638-by-876 pixels. Figure 2 shows images taken for one subject. A total of 136 images were taken for 18 subjects. These gray scale images are then converted to binary images with threshold. The wrist of hand is removed using morphological operators and then the hand boundary is traced to calculate the centroid. Theoretically, the maximum distance point on the boundary from centroid is the middle finger tip. This point along with centroid is used to determine optimal angle for Radon transform. Figure 3b shows the intensity histogram of the sample image of Figure 3a. The image in Figure 3a is first converted to double format within range [0,1] before calculating its histogram. The threshold problem is substantially simple in this case as the images were taken against dark background. As we can see the foreground (gray) pixels are well separated from the background pixels at an intensity value of 0.15. Thus a threshold value T = 0.15 is chosen and this value is well for all the images in the data set. Any intensity value greater than T is assigned the value ‘1’ and anything lower than that is thresholded to ‘0’. Figure 3c shows the thresholded binary image. Notice the

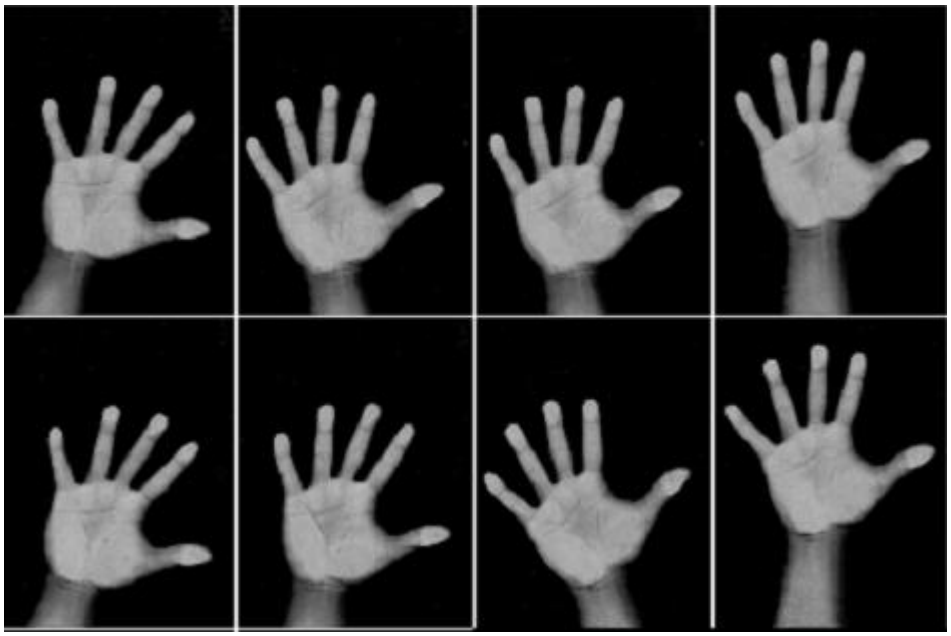

Figure 2. Example of collected hand images.

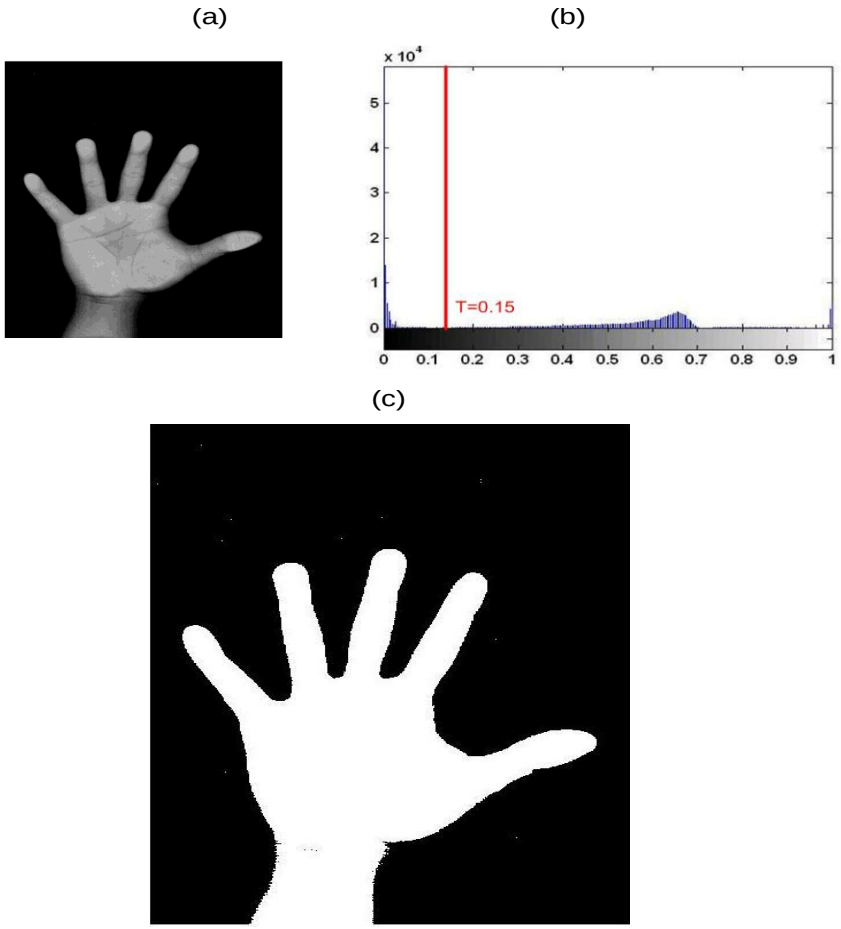

Figure 3. (a) Gray scale hand image **(b)** Determination of threshold value from intensity histogram **(c)** Obtained binary image.

small isolated white pixels on the dark background. Those pixels are removed while operating the morphological structures to eliminate wrist.

Removal of wrist-morphological operation

The success of the proposed method largely depends on the correct location of the palm centroid. For that we must erase the wrist portion from the hand image. This is done by morphological operations. A series of morphological opening with disk type structuring element followed by logical 'exclusive or' operation is performed to eliminate wrist. The morphological opening for binary images can be defined as

$$A \circ B = \bigcup \{ (B)_z \mid (B)_z \subseteq A \} \quad (5)$$

where $\bigcup\{.\}$ denotes the union of all sets inside the braces, and the notation $B \subseteq A$ means that B is a subset of A. The notation $(B)_z$ represents the translation of B to a point $z \equiv (z_x, z_y)$. The morphological opening removes all the foreground pixels that are smaller in size than the structuring element. In this application the disk type structuring element was chosen with radius 100.

Centroid of hand

After the morphological operations on the wrist, a contour of a hand is obtained. With the discrete parametric equation in Cartesian coordinate system, the closed curve of the hand can be expressed as

$$\Gamma(n) = (x(n), y(n)) \quad (6)$$

where $n \in [0, N-1]$; the hand may be parameterized with any number N of vertices and $\Gamma(N) = \Gamma(0)$. The centroid of the closed polygon of the hand defined by N vertices (x_i, y_i) can be calculated in terms of its area and vertices as below. The area A

$$A = \frac{1}{2} \left| \sum_{i=0}^{N-1} (x_i y_{i+1} - x_{i+1} y_i) \right| \quad (7)$$

and its centroid is $C \equiv (C_x, C_y)$ where

$$C_x = \frac{1}{6A} \sum_{i=0}^{N-1} (x_i + x_{i+1})(x_i y_{i+1} - x_{i+1} y_i) \quad (8)$$

$$C_y = \frac{1}{6A} \sum_{i=0}^{N-1} (y_i + y_{i+1})(x_i y_{i+1} - x_{i+1} y_i) \quad (9)$$

Note that the polygon has to be closed, that is, the vertex (x_N, y_N) is assumed to be the same as (x_0, y_0). One can notice that the position of the centroid in Figure 4 is fixed no matter how the points distribution is. So using Equations 8 and 9, we can obtain the genuine centroid of a contour under whatever the contour is normalized. The dots are points distributed on the contour uniformly (a) and non-uniformly (b). The star is the centroid of original contour and the inner dot is the centroid of sampled contour.

Finger tip identification

Identification of the middle finger tip is an important step of this method. This point along with the centroid, which is the center of mass of the palm, is used to determine the angle parameter for calculation of Radon Transform. That means these two points provide the direction along which the line integral (projection) has to be taken. Figure 5 shows the result for the wrist-morphological operation along the direction of the line integral. After the successive morphological operations, the palm centroid (C_x, C_y) is calculated as in equations 8 and 9. Now the maximum centroid distance of the hand boundary corresponds to the middle finger tip. This point will be called 'control point' in the subsequent sections.

This middle finger tip point is denoted as $(CTRL_x, CTRL_y)$. In order to calculate centroid distance we first need to trace the hand boundaries. The boundary is traced using eight connected neighborhoods. This process is described in Amayeh et al. (2006) in detail. Figure 6 (a) shows a traced binary hand image. Figure 6 (b) shows the centroid and control points marked by red dots. The control point is found by locating the maximum centroid distance as shown in Figure 6 (c).

Translation and rotation invariant feature vectors

The Radon transform has low computational cost and is effective to recognize the palm shape even in case of disjoint palm images or palm images with holes. However the transform is sensitive to translation and rotation as shown in equations 3 and 4.

First, to solve the translation sensitive problem, the translation invariant feature vectors are required. This problem can be solved by using the shifting property in equation 3 by replacing the palm centroid (C_x, C_y) with the origin (x_0, y_0). By assigning $(C_x, C_y) \equiv (x_0, y_0)$ to $(0,0)$ for the whole palm images, the equation 3 can be represented with

$$R[f(x - x_0, y - y_0)] = R(\rho - x_0 \cos\theta - y_0 \sin\theta, \theta) = R(\rho, \theta) = R[f(x, y)] \quad (10)$$

Secondly, the rotation variant problem can be solved by using the rotation property in equation 4 by replacing the angle $\theta - \phi$ with the fixed angle θ_{fixed}. With the reference of this fixed angle, all data points on the binary palm image are placed in the new position. After then, the equation 4 can be expressed with

$$R[f(x', y')] = R(\rho, \theta - \phi) = R(\rho, \theta_{fixed}) \quad (11)$$

Here, the fixed angle for radon transform is defined by simply calculating the slope of the line connecting the palm centroid (C_x, C_y) and the middle finger tip control point $(CTRL_x, CTRL_y)$. The angle $\theta_{optimal}$ can be written mathematically as (in degrees)

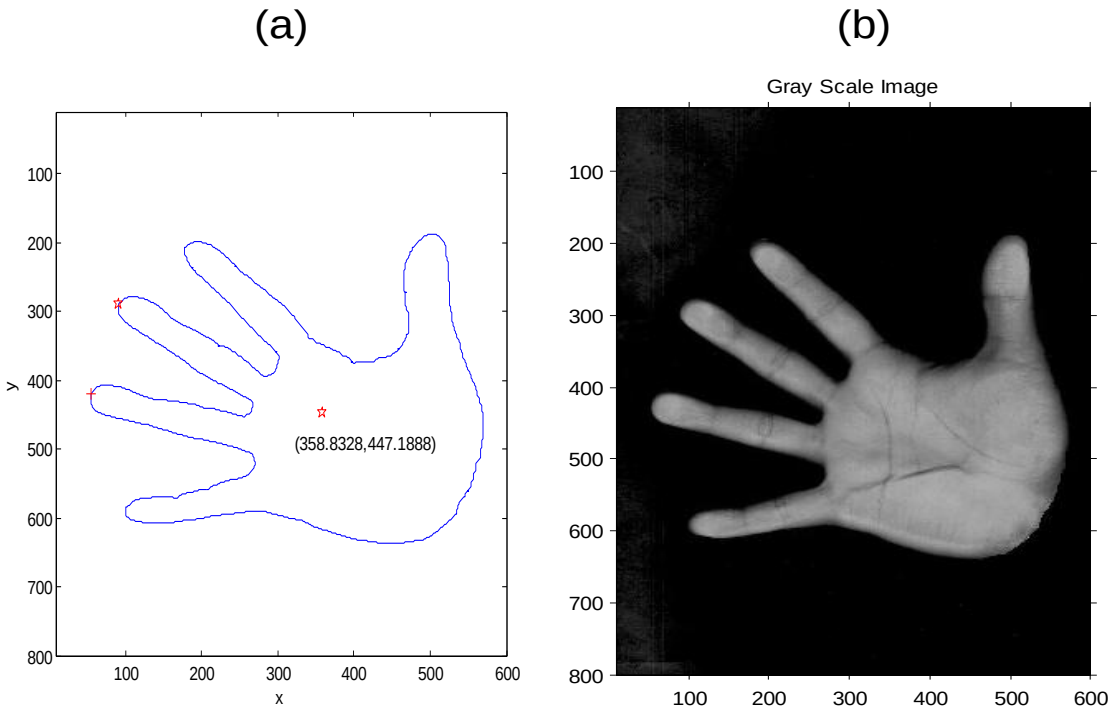

Figure 4 (a). Gray scale hand image (b) Centroid position corresponding to Figure 4a.

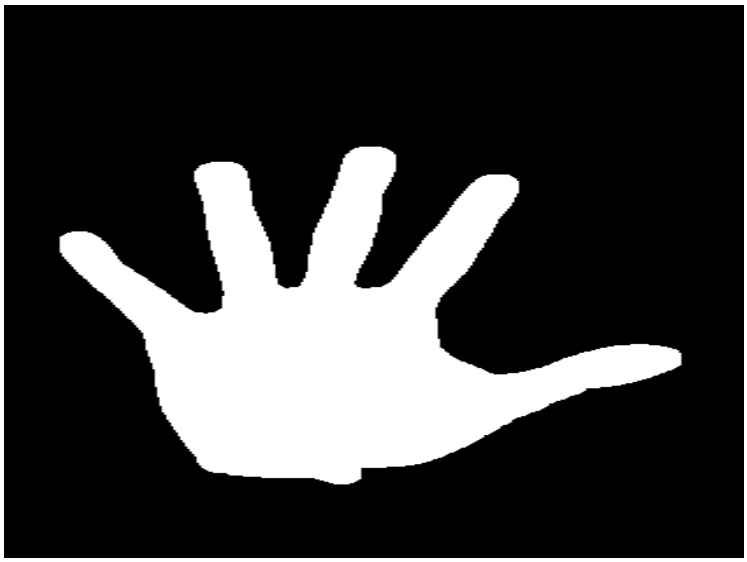

Figure 5. Elimination of wrist after successive morphological operations.

$$\theta_{optimal} = \begin{cases} \tan^{-1}\dfrac{B}{A} & when\ B\ and\ A\ have\ same\ sign \\ 180^{o} + \tan^{-1}\dfrac{B}{A} & when\ B\ and\ A\ have\ opposite\ signs \end{cases} \quad (12)$$

with $A = CTRL_x - C_x$ and $B = CTRL_y - C_y$.

The angle $\theta_{optimal}$ is assigned to be the constant fixed angle θ_{fixed}. With the reference of this fixed angle, all data points on the binary palm image are rotated by $\theta_{optimal} - \theta_{fixed}$ counter-clockwise around the palm centroid.

The translation and rotation invariant feature vectors can be achieved through the equations (10) and (11). From these

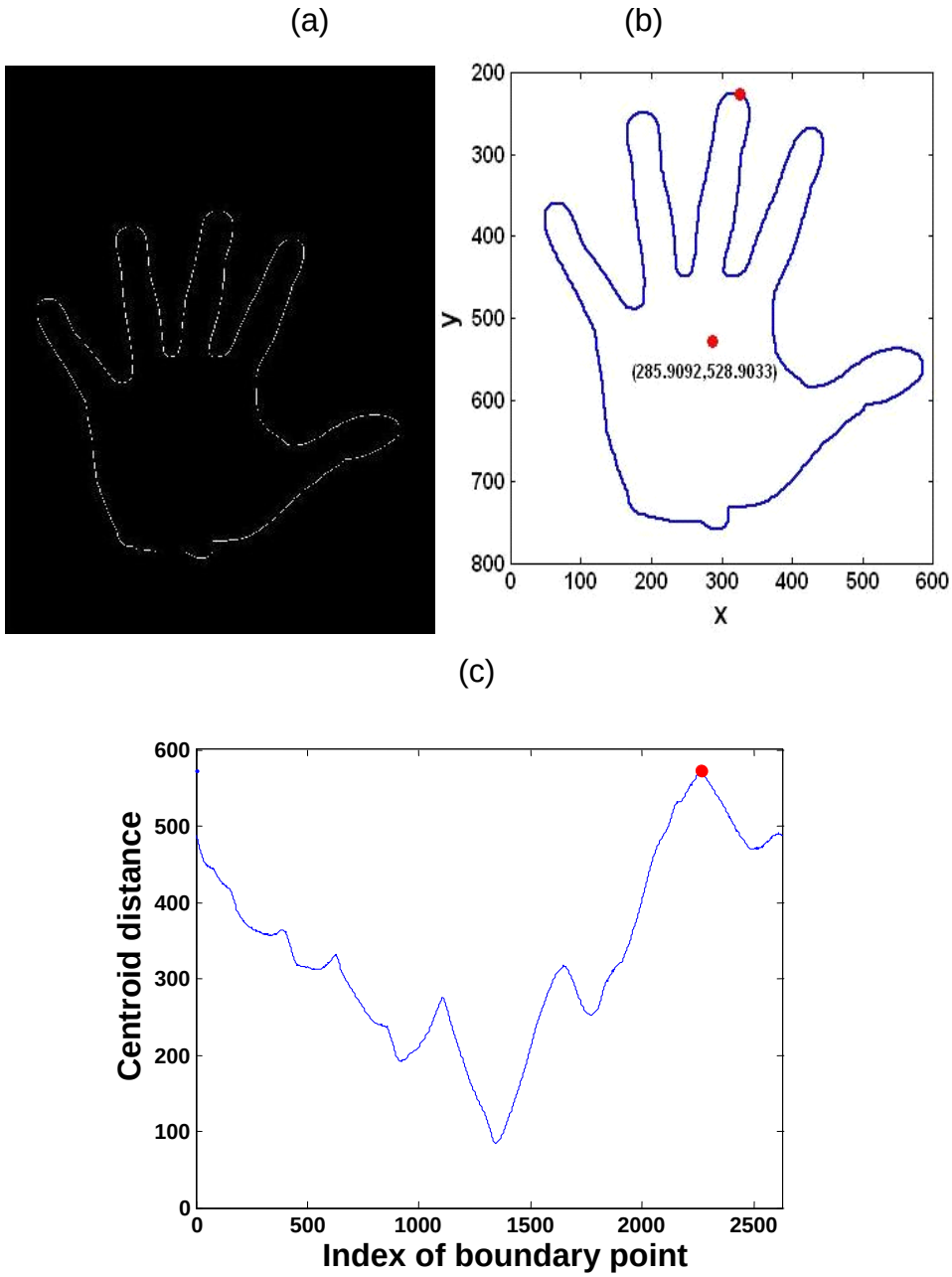

Figure 6 (a). Traced boundary of hand **(b)** Location of palm centroid and control point **(c)** The centroid distance profile (The dot corresponds control point).

equations, one can see that the proposed scheme is robust to translation and rotation and suitable for the peg free hand shape authentication. Figure 7 shows the procedure to achieve the translation and rotation invariant feature vectors.

In order to recognize a palm image correctly, one uses the translation and rotation invariant feature vector which can be not only useful for recognition, but also generate matching scores. Quality matching scores reflect the relative matching proximity between the instances of a palm image class. To capture the maximum proximity of matching between the translation and rotation invariant feature vectors, we use the similarity measurement techniques for generating matching scores with Euclidean distance. The matching score for feature vectors is defined as follows

$$S = 1 - \frac{\|X - Y\|}{\|X\|} \tag{13}$$

where X and Y denotes 'gallery' and 'probe' feature vectors respectively. $\|X - Y\|$ represents Euclidean Distance between them. $\|.\|$ denotes Euclidean norm.

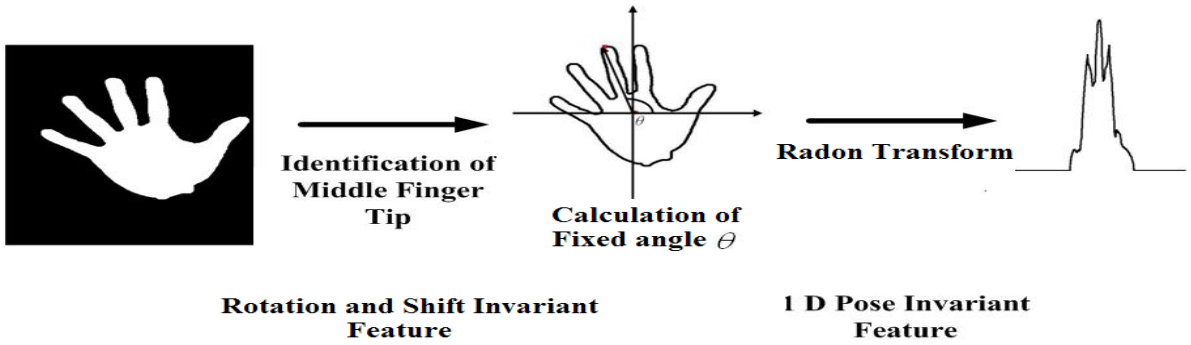

Figure 7. Procedure to achieve the translation and rotation invariant feature vectors.

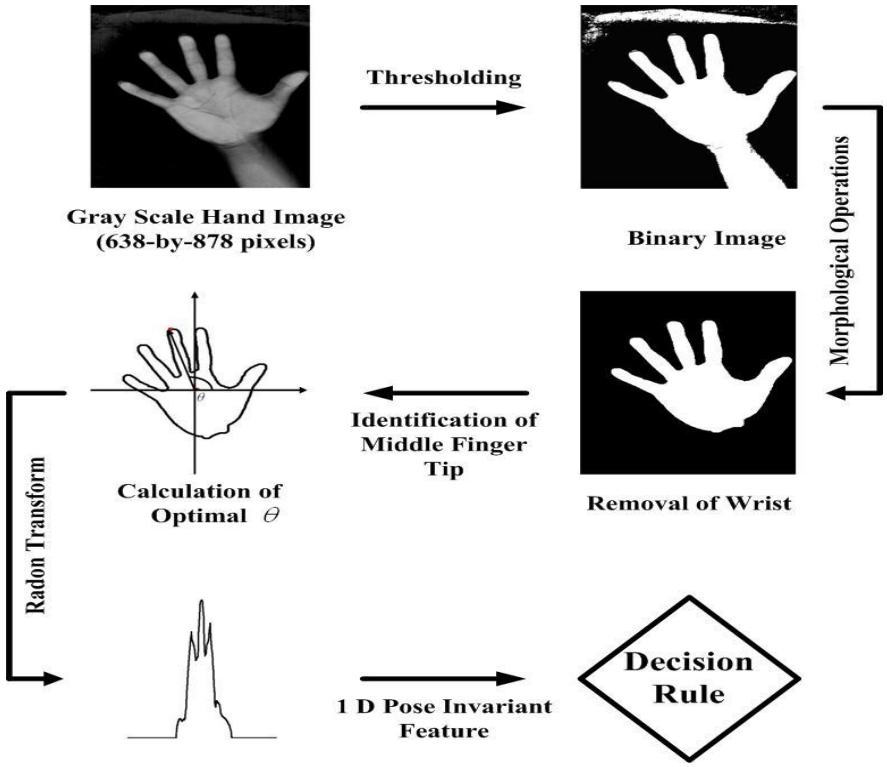

Figure 8. Flow diagram of the proposed method.

Finally, the block diagram of a palm authentication is shown in Figure 8. The link between feature vector extraction and the decision rule was established by calculating matching score in equation 13.

EXPERIMENTAL RESULTS

Translation and rotation invariant test

For the experiments we have collected palm images of 30 users gesturing the 326 different postures (Figure 9). Leaving one gallery image per person, we have a total of 30 probe images. The palm images were captured with a document scanner against a dark background. 75 dpi images were taken in 8 bit gray scale format. Each image has a size of 638-by-876 pixels.

To test the robustness of our fixed angle radon transformation scheme, we performed various translation and rotation experiments for a single palm. Figure 9 shows experimental results of the proposed fixed angle radon transform with the same palm under the different posture. Figure 9a and b show an original palm image and a corresponding feature vector respectively. First, to investigate the translation invariant feature of the fixed radon transform, we simply give the 290 pixels shift to the x and y coordinates of the position of hand location as

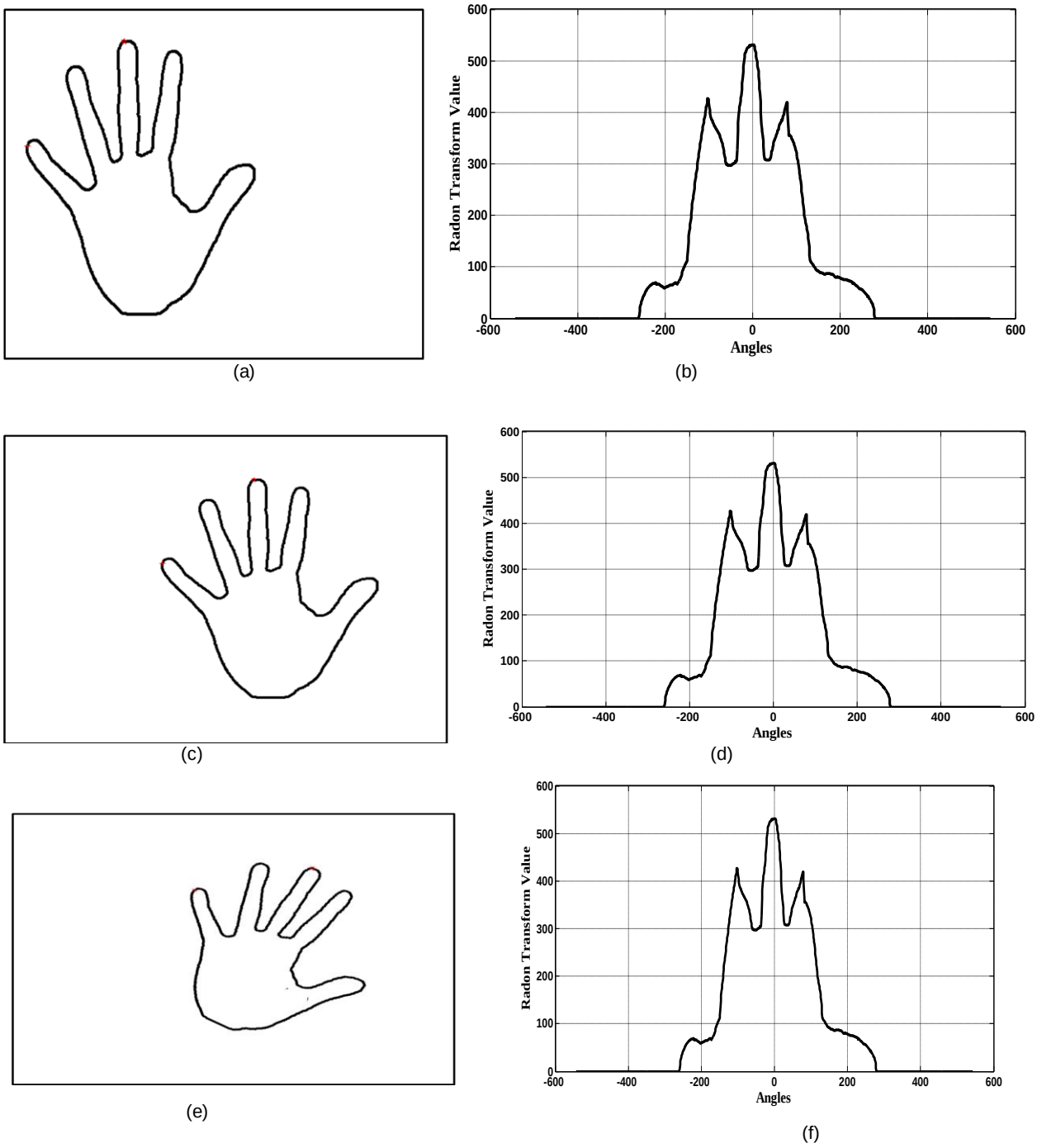

Figure 9. Translation and rotation invariant test experiments for a single palm (a) A hand image; (b) Corresponding feature vector for figure 9(a); (c) 290 pixels translated hand image; (d) Corresponding feature vector for figure 9(c); (e) 45°clockwise rotated hand image; (f) Corresponding feature vector for figure 9(e).

shown in Figure 9c. Under this condition, the fixed angle radon transform is performed. The experimental result demonstrates that the feature vector of Figure 9d is same with the feature vector as shown in Figure 9b. It verifies that the proposed fixed angle radon scheme has a translation invariant property. Secondly, to investigate the rotation invariant feature of the fixed radon transform, we simply give the rotation of 45° in the original image leads to the phase shift of 45° in Radon Transform. Under this condition, the fixed angle radon transform is performed. The experimental result shows that the fixed radon transform feature vector was not changed as shown in

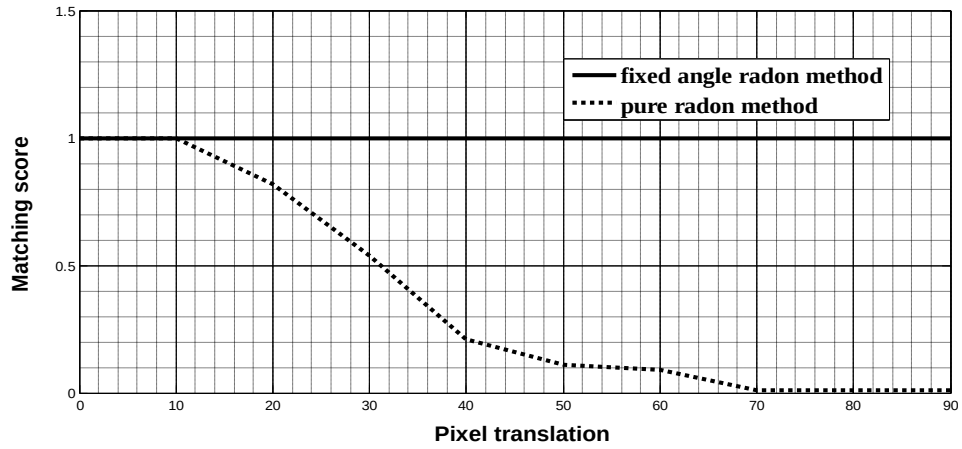

Figure 10. Matching score versus amount of translation for the fixed angle radon method, and the pure radon transform method. The x-axis is the amount of translation, in pixels, applied to both the x and the y dimensions of the test palm image, The y-axis is the matching score for feature vectors obtained by each method.

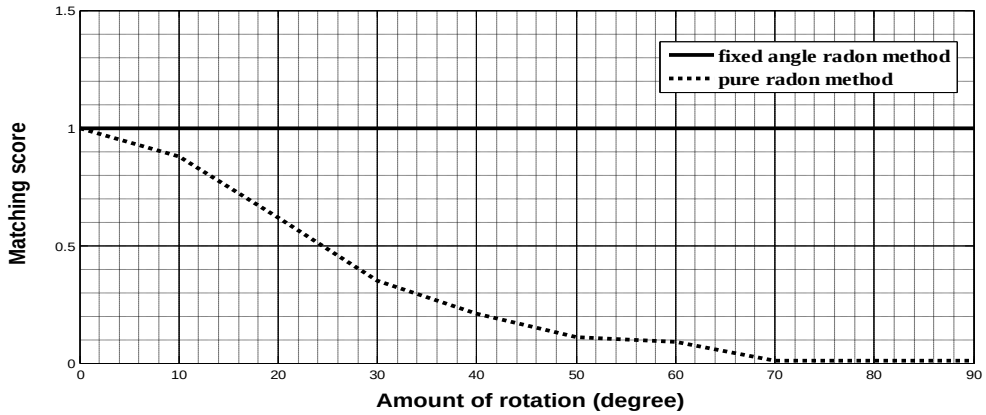

Figure 11. Matching score versus amount of rotation for the fixed angle radon method, and the pure radon transform method. The x-axis is the amount of rotation, in degrees, applied to the test palm image, the y-axis is the matching score for feature vectors obtained by each method.

Figure 9b and f. We can see that the rotation invariant problem can be solved with the fixed angle $\theta_{optimal}$. Therefore, the fixed angle radon transform is invariant under translation and rotation if we resize the image into a normalized scale, which is feasible in a peg free hand authentication. For each palm image, the 360-by-1 dimensional feature vector, instead of the 638-by-876 pixel matrix, is extracted to represent the shape of the palm under the fixed angle radon transformation. The information that the silhouette carry is transformed in a more compact way and invariant to geometry transformation.

To apply a certain amount of translation to the input palm postures for subjects gesturing the different postures, we simply add 10 pixels up to 90 pixels the x and y coordinates of the position of each candidate hand location since the whole each image has a size of 638-by-876 pixels. Moreover, to apply a certain amount of rotation to the input palm postures, we simply rotate the x and y coordinates of each candidate hand location by 10° up to 90°. In Figures 10 and 11, the experimental results show how the matching score of each method varies as we artificially translate and scale the test palm images for 30 subjects. Figure 10 shows the average matching score versus amount of translation for the fixed angle radon method, and the pure radon transform method. Figure 11 shows the average matching score versus amount of rotation for the fixed angle radon method, and the pure radon transform method. Naturally, as the method proposed in this paper is invariant to translation and rotation, the matching score of our method is not affected at all by this artificial translation and scaling. In contrast, the pure radon transform without the fixed angle

and centroid shift can only tolerate relatively small amount of translation and rotation, with performance rapidly deteriorating as larger amounts of translation and rotation are used.

Personal identification experiment

Performance of a biometric system is measured by False Acceptance Rate (FAR) and False Rejection Rate (FRR). To complete tradeoff curve over many operating points (threshold values) for numerous hand images, the biometric performance index, FAR and FRR defined as follows, have been evaluated.

$$FAR = \frac{Number\ of\ accepted\ imposters}{total\ number\ of\ imposters} \times 100\ \% \quad (12)$$

$$FRR = \frac{Number\ of\ rejected\ \ jenuines}{total\ number\ of\ \ jenuines} \times 100\ \% \quad (13)$$

It is used to measure and to compare the performance among several biometric systems. Personal identification is a process to identify a person who is registered to a system. A test data (gallery data) must be compared to all probe data stored in the database. This step can be handled by the matching scores in equation 13. The system then decides from the matching scores who the person is. Normally, in order to calculate FAR and FRR, a score threshold must be set. If the matching score is more than threshold, the system will reject the attempting person. For the experiment, a total of 136 images were captured. Leaving one gallery image per person, we have a total of 18 probe images. The distribution of FAR and FRR with different threshold is showed in Figure 12a. They cross-over at threshold value 0.82. Figure 12(b) shows the Receiver Operating Characteristics (ROC) curve. The equal Error Rate 5.1% is obtained at threshold value 0.82.

In Jain et al. (1997) around 360 images were tested and a false acceptance rate (FAR) of 2% and a false rejection rate (FRR) of 15% were obtained. A database of 200 hand images from 20 people was tested in Gunther (2002) and 97% success in identification and error rates below 10% in verification was reported. These two data sets are large enough to be considered impressive. Oden et al. (2003) reported 95% success in identification and 99% success in verification using 40 images. However this population is not that impressive although success rate is very high. Jain et al. (1999) developed a verification system with 353 images based on alignment of finger contours and measured the mean alignment error between them. Their reported FAR and FRR were of 2 and 3.5% respectively. The paper presented here established an Equal Error Rate of 5.1%. Comparing with the research of Jain et al. (1997), the FRR is 10% less. It also has better verification result than Gunther (2002). The

(a)

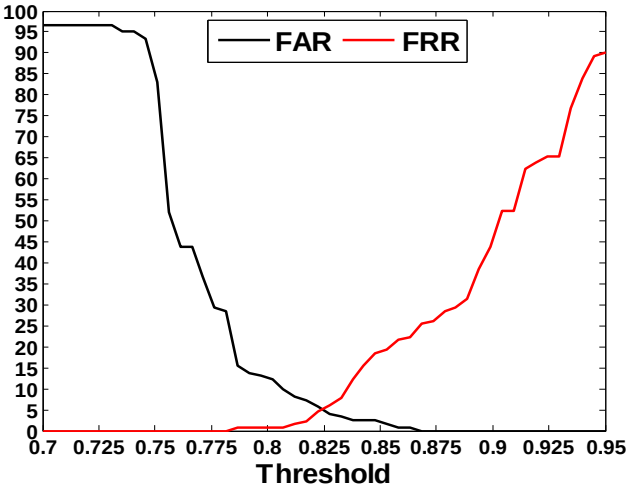

(b)

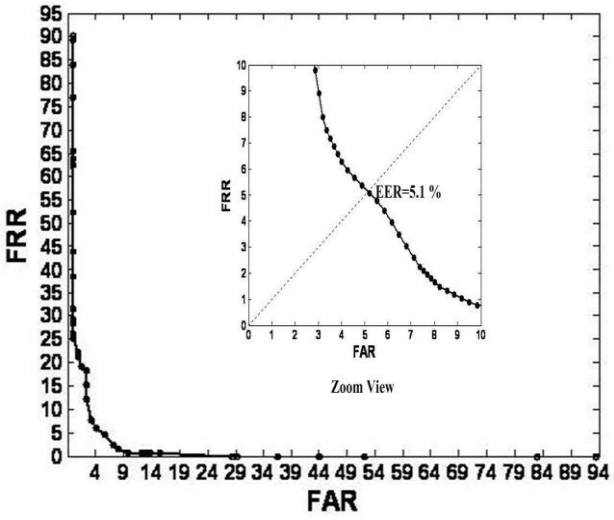

Figure 12(a). Genuine and imposter distribution **(b)** ROC curve. The Equal Error Rate is 5.1%.

The data set used (136 images) in this paper is moderate in size. However, the similar results are expected for a larger data set.

Conclusion

A novel method for hand shape verification using the fixed angle radon transform and centroid is proposed in this paper. Instead of measuring the lengths and widths, this method extracts position invariant features for hand shape. That also facilitates peg free operation. Low resolution images obtained with a simple document scanner exhibits an impressive 5.1% error rate. To make

the computation radon transform feasible, we presented a new algorithm that avoids redundant computations to speed up things and uses arbitrary precision arithmetic to ensure accurate moment computations. Experimental results demonstrate that the proposed scheme is invariant to translation and rotation, the matching score of our method is not affected at all by this artificial translation and scaling. In contrast, the pure radon transform without the fixed angle and centroid shift can only tolerate relatively small amount of translation and rotation, with performance rapidly deteriorating as larger amounts of translation and rotation are used. Using a database of 136 images from 18 subjects, the distribution of FAR and FRR with different threshold have analyzed. The equal Error Rate 5.1% is obtained at threshold value 0.82. Qualitative comparisons between the proposed scheme and other systems demonstrate that our system performs comparable or better. Then, verification can be performed by just considering information from the fingers, the palm or both. Such an approach would tolerate finger motion and completely remove the requirement to place the hand in a stretched position. Finally, we plan to test the robustness of the method when there is substantial passage time between the template and test images.

REFERENCES

Amayeh G, Bebis G, Erol A, Nicolescu M (2006). “Peg-Free Hand Shape Verification Using High Order Zernike Moments,” Computer Vision and Pattern. Recognition Workshop (2006). CVPRW '06. Conference on, 17-22 June 2006, pp. 40-40.

Ernst RH (1971). “Hand ID system,” US Patent No. 3576537.

Gonzalez RC, Woods RE, Eddins SL (2004). Digital Image Processing Using Matlab, second edition, Prentice Hall, Upper Saddle River, New Jersey, pp. 334-350.

Gunther M (2002). “Device for identifying individual people by utilizing the geometry of their hands,” European Patent No. DE10113929.

Han CC, Jang BJ, Shiu CJ, Shiu KH, Jou GS (2002). “Hand features verification system of creatures,” European Patent No. TW476917.

Hansen KV, Toft PA (1996). “Fast Curve Estimation Using Preconditioned Generalized Radon Transform,” IEEE Trans. Image Processing, 5(12): 1651-1661.

Jacoby IH, Giordano AJ, Fioretti WH (1972). “Personal identification apparatus,” US Patent No. 3648240.

Jain AK, Ross A, Pankarti S (1997). “A prototype hand geometry based verification system,” in Proc. 2nd Internat. Conf. on Audio Video based Biometric Personal Authentication, March 1999, pp. 166–171.

Kumar A, Wong DC, Shen HC, Jain AK (2006). “Personal authentication using hand images,” Pattern Recogn. Lett., 27(13): 1478-1486.

Miller RP (1971). “Finger dimension comparison identification system,” US Patent No. 3576538.

Oden C, Ercil A, Buke B (2003). “Combining implicit polynomials and geometric features for hand recognition,” Pattern Recognition Lett. 24: 2145–2152.

Sanchez-Reillo R, Sanchez-Avila C, Gonzales-Marcos A (2000). “Biometric identification through hand geometry measurements” IEEE Trans. Pattern Anal. Machine Intell., 22(10): 1168–1171.

Sidlauskas DP (1988). “3D hand profile identification apparatus” US Patent No. 4736203.

Wong ALN, Shi P (2002). “Peg-Free Hand Geometry Recognition Using Hierarchical Geometry and Shape Matching,” IAPR workshop on Machine Vision Applications, pp. 281-284.